Cervical tooth anatomy considerations for prefabricated anatomic healing abutment design: A mathematical formulation

Article *in* Journal of Prosthetic Dentistry · January 2021

DOI: 10.1016/j.prosdent.2020.11.023

CITATIONS
3

READS
959

5 authors, including:

János Vág
Semmelweis University
83 PUBLICATIONS **796** CITATIONS
SEE PROFILE

George Freedman
BPP University College
1,068 PUBLICATIONS **582** CITATIONS
SEE PROFILE

Eniko Vaszine Dr. Szabó
Semmelweis University
18 PUBLICATIONS **190** CITATIONS
SEE PROFILE

G. Berkei
Helvetic Clinics
6 PUBLICATIONS **16** CITATIONS
SEE PROFILE

THE JOURNAL OF PROSTHETIC DENTISTRY

CLINICAL RESEARCH

Cervical tooth anatomy considerations for prefabricated anatomic healing abutment design: A mathematical formulation

János Vág, DMD, PhD, Dr habil,[a] George Freedman, DMD,[b] Enikő Szabó, DMD, PhD,[c] László Románszky, CDT,[d] and Gábor Berkei, DMD[e]

ABSTRACT

Statement of problem. A custom emergence profile offers the ideal horizontal dimensions for an anatomic healing abutment. However, developing such an emergence profile can be a time-consuming and complex process.

Purpose. The purpose of this study was to develop a mathematical formula defining horizontal cervical tooth geometry to design prefabricated, tooth-specific, healing abutments.

Material and methods. Cone beam computed tomography (CBCT) horizontal cross sections of 989 teeth on 54 participants were measured. For anterior and premolar teeth, 2 perpendicular ellipses were fitted onto the cervical tooth cross section that was defined by 3 parameters. The lingual ellipse followed the lingual outline of the tooth, and its diameter was the largest mesiodistal diameter of the tooth (parameter "a"); its buccolingual radius became parameter "b." The buccal ellipse was perpendicular to the lingual ellipse and followed the buccal outline of the tooth. The buccolingual radius of the smaller ellipse became parameter "c." For molars, the first ellipses followed the mesial outline of the tooth, and its larger diameter (parameter "a") matched the largest buccolingual diameter of the tooth. Its smaller radius became parameter "h1." The second ellipse was parallel to the first ellipse and followed the distal outline of the tooth. Its larger diameter became parameter "b", and its mesiodistal diameter became parameter "h2". Statistical differences between parameters were evaluated by the linear mixed model (α=.05 after Bonferroni adjustment). Pairwise comparisons were made separately for each parameter of the molars and separately for each parameter for the anterior teeth plus premolars. Teeth were put into the same parameter cluster if no significant differences were found between them for a specific parameter. If neither parameter (4 for molars and 3 for the other teeth) was different for 2 teeth, they were put into the same abutment cluster. The abutment clusters determined the type of anatomic healing abutment. The areas were calculated from the developed mathematical formula by using the parameters. In addition, cervical areas of 106 randomly chosen teeth were measured directly with a photo-editing software program. A computer algorithm was used to select 5 CBCT scans from the 54 by using the simple randomization method. The agreement between the 2 methods was evaluated by Bland-Altman analysis.

Results. The lower and upper limits of agreement between the 2 methods were -8.57 and 7.36 mm^2, respectively, with no bias (-0.61 mm^2, P=.224). Significant differences were found between most parameters among the 14 tooth types (P<.001). Based on the parameters, 12 specifically distinct clusters were defined. Two tooth types were pooled into 1 abutment cluster: the maxillary first and second premolars and the mandibular first and second molars.

Conclusions. The cervical tooth cross section can be accurately defined by combining 2 elliptical elements. A comprehensive array of tooth specific emergence profiles can be provided by just 12 different prefabricated abutments, designed as per the recommended parameters. (J Prosthet Dent 2020;■:■-■)

More than 800 000 implants are installed in the United States annually and more than 1.8 million in the European Union.[1] As well as providing function, implant-supported restorations should restore the esthetics of the teeth being replaced and have emergence profiles and contours that facilitate oral hygiene.[2-4]

Support provided by the following fundings: The National Research, Development, and Innovation Office (KFI_16-1-2017-0409) and The Hungarian Human Resources Development Operational Program (EFOP-3.6.2-16-2017-00006) covered the cost of consumable materials and software. Additional support was received from the Thematic Excellence Program (2020-4.1.1.-TKP2020) of the Ministry for Innovation and Technology in Hungary, within the framework of the Therapy thematic program of the Semmelweis University.

[a]Associate Professor, Department of Conservative Dentistry, Faculty of Dentistry, Semmelweis University, Budapest, Hungary.
[b]Adjunct Professor, Schulich School of Medicine & Dentistry, Western University, Toronto, Canada.
[c]Assistant Professor, Department of Conservative Dentistry, Faculty of Dentistry, Semmelweis University, Budapest, Hungary.
[d]Dental Technicians, Artifex Dentis, Budapest, Hungary.
[e]Private practice, Helvetic Clinics, Revay Dental Clinic, Budapest, Hungary.

Clinical Implications

The novel mathematical algorithm provides a robust method for the high scale measurement of cervical tooth geometry. The parameters calculated in this study could be used to design accurate anatomic healing abutments to facilitate the shaping of the emergence profile.

Accurate implant placement is essential for optimal esthetics, and the apicocoronal, faciolingual, and mesiodistal parameters of implant placement have been well described.[5,6] The optimal implant diameter, as well as the morphology of the abutment, is dependent on the cervical dimension of the natural tooth to be replaced.[7,8] This information is also critical to achieving a maintainable and realistic soft tissue morphology.[9,10]

Prefabricated circular healing abutments promote nonanatomic soft-tissue maturation that must be remedied at the restorative stage by the judicious and clinically sensitive addition of resin to the interim crown and abutment.[6,11-13] However, the soft tissue healing time[14,15] and the limits of immediate tissue compression[16,17] make the task of developing a clinically correct emergence profile a time-consuming, demanding, multistep process both chairside and in the dental laboratory.[18-20] Incompletely polymerized shape-modifying resin may also cause soft tissue irritation in some patients.[21,22]

These common clinical challenges can be readily overcome by using tooth-specific, anatomically designed, prefabricated healing abutments that mimic natural tooth geometry instead of prefabricated circular healing abutments. In the 1990s, the Bio-Esthetic Abutment System was designed and marketed by Steri-Oss with an anatomically shaped healing and prosthetic abutment to overcome this challenge.[23,24] Unfortunately, the Bio-Esthetic Abutment System is no longer available, but 3 different anatomic healing abutment systems are currently commercially available: Cervico VPI (VP Innovato Holdings LTD), Anatotemp (Buckeye Medical Technologies LLC), and Contour Healer (Contour Healer LLC). These systems are simplified and schematic, and their design parameters have not been published. Cervical diameter data have been published, but these studies assumed a standardized symmetric and circular cross-sectional morphology for all tooth types.[7,8,25] A straightforward mathematical algorithm is needed to reconstruct the cervical cross-sectional shape of each tooth type (anterior, premolar, and molar) to enable the fabrication of accurate anatomic healing abutments. Ideally, the algorithm would involve a manageably limited number of parameters, and the calculation-predicted cross-sectional area would closely match the cross-sectional area of the original tooth.

The purpose of this study was to develop a mathematical algorithm based on the known cross-sectional geometry of each tooth type at the cementoenamel junction (CEJ).[26] An additional purpose was to validate the algorithm by evaluating the agreement between the calculated cross-sectional area and a direct measurement on cone beam computed tomography (CBCT) scans and to make highly accurate measurements for the cervical cross-sectional dimension with an estimate of the mean of each parameter for each tooth type. The null hypotheses were that the cross-sectional geometry calculated by a mathematical algorithm would not differ from the direct area measurement and that no significant difference would exist in the parameters describing the cross-sectional geometry among tooth types.

MATERIAL AND METHODS

Fifty-four white participants (28 women and 26 men) aged 20 to 70 years who had had CBCT scans made for treatment purposes were enrolled in the study. A total of 989 tooth cross sections were measured, 35 teeth per tooth type on average. Exclusion criteria included anatomic or developmental anomalies, teeth with extensive restorations, and restorations involving the cervical region. Each study participant received written information about data usage and signed an informed consent. The study was carried out in accordance with the Declaration of Helsinki, with the approval of the Committee Health Registration and Training Center (permission number: ETT TUKEB 31293-3/2018/EKU).

Scans (8×8 cm volume) were made with a CBCT unit (ProMax 3D Max CBCT; Planmeca) with 90 kV, 8 mA, 15.02 second exposure time, and 1138 dose area product with a pixel size of 150 μm. For each tooth, the longitudinal axis and a plane perpendicular to it were defined at the buccal CEJ in a software program (Romexis v4.6.2.R; Planmeca) (Fig. 1A). The cross section at this plane was visualized (Fig. 1B, 1C), and the distance measurements were made directly in the CBCT software program. A computer algorithm was used to select 5 CBCT scans from the 54 randomly. No additional factor was assessed during the procedure; thus, it matched the simple randomization method.[27] The cross sections of 106 teeth of the 5 selected study participants were outlined and exported to a photo-editing software program (Adobe Photoshop CC v20170425.r.252 x64; Adobe Inc).

Distance measurements were used to obtain area calculation parameters. Two formulas were developed. For the anterior teeth (incisors, canines) and premolars, the area calculation was developed by projecting 2 ellipses on the cross section of the tooth (Fig. 1D). The lingual ellipse followed the lingual outline of the tooth,

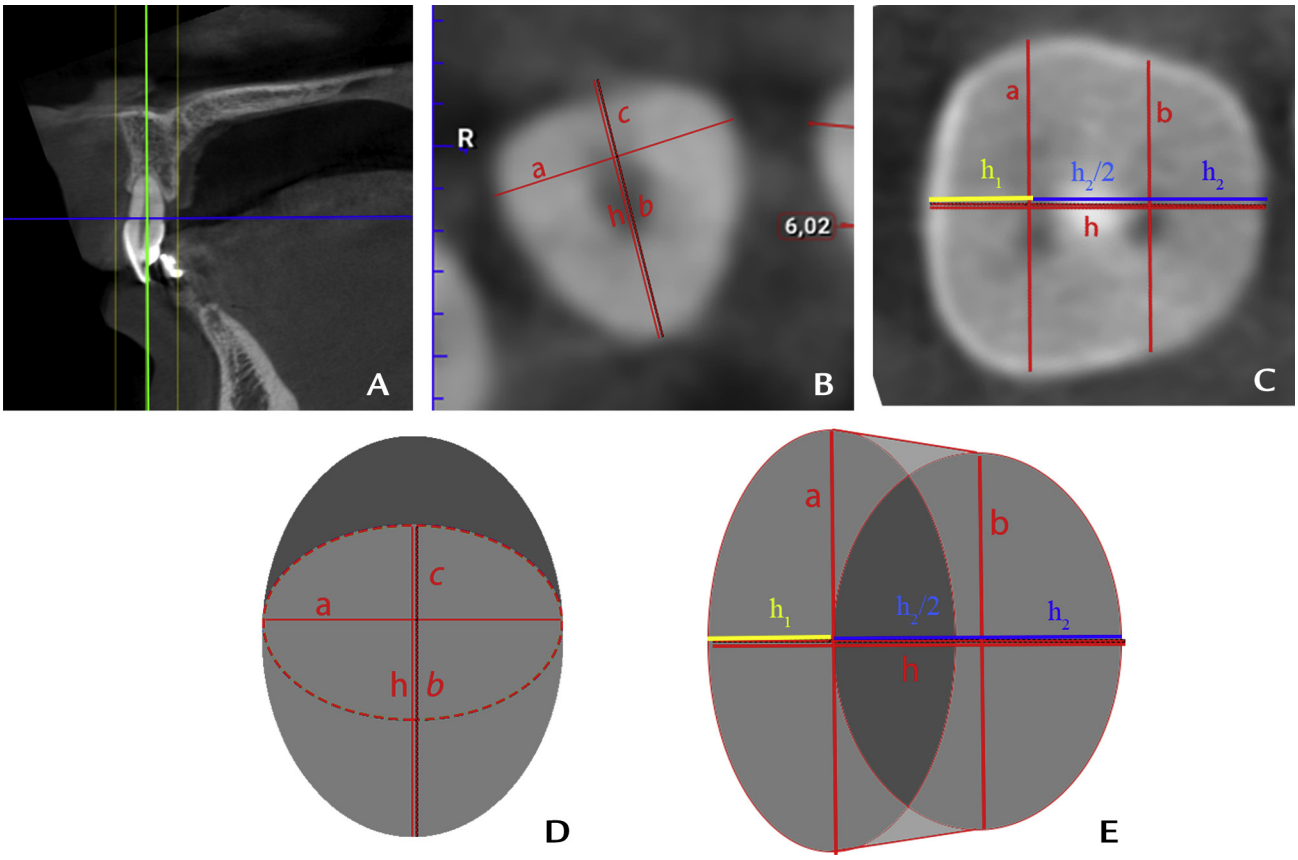

Figure 1. Analysis of cervical tooth cross-sections. A, Selection of longitudinal axis (*green* line) and setting perpendicular plane to it (*blue* line) at buccal cementoenamel junction level. B, Cross section of maxillary central incisor and measurement of 3 related parameters; a, b, c. C, Cross section of maxillary first molar and measurement of 3 related parameters; a, b, c, h_1, h_2. D, Geometry of anterior teeth and premolars simplified by 2 perpendicular ellipses. Smaller ellipse defined by radius c and diameter a, larger ellipse defined by radius b and diameter a. h=c + b. E, Geometry of molars simplified by 2 parallel ellipses. Mesial defined by radius h_1 and diameter a and distal defined by radius $h_2/2$ and diameter b.

and its diameter was the largest mesiodistal diameter of the tooth (parameter a) and its buccolingual radius was parameter b. The buccal ellipse was perpendicular to the lingual ellipse and matched its diameter (parameter a). The buccal ellipse followed the buccal outline of the tooth. The buccolingual radius of the smaller ellipse was parameter c. The area of the anterior, canine, or premolar tooth was calculated by the sum of the half area of the 2 ellipses as follows:

$$\text{Area} = \frac{\frac{a}{2}\times c\times\pi}{2} + \frac{\frac{a}{2}\times b\times\pi}{2}.$$

For the molar teeth, the area calculation was defined by projecting 2 partially overlapped parallel ellipses on the cross section of the tooth (Fig. 1E). The first ellipse was the largest buccolingual diameter of the tooth (parameter a). The smaller radius (parameter h_1) was the section of the mesiodistal diameter of the tooth, which extended between the perimeter and the largest buccolingual diameter of the tooth. The second ellipse was parallel to the first ellipse, and its larger diameter was the buccolingual diameter of the tooth (parameter b) where it perpendicularly intersected the mesiodistal diameter of the tooth (parameter h) at a specific point at the middle of the larger part of the mesiodistal diameter (parameter h_2). Thus, it divided h_2 into 2 equal segments (parameter $h_2/2$). The shorter diameter of the second ellipse was the section of the mesiodistal diameter of the tooth, which extended between the perimeter of the tooth and the b diameter. The 2 ellipses were connected by 2 tangent lines to each other. The area of the molar tooth was calculated as follows:

$$\text{Area} = \frac{\frac{a}{2}\times h1\times\pi}{2} + \frac{\frac{b}{2}\times\frac{h2}{2}\times\pi}{2} + \left(\frac{a+b}{2}\times\frac{h2}{2}\right).$$

The cross sections were transferred from the CBCT scan to the photo-editing software program. Distance measurements were included for calibrating the image with the Measurement Log panel, while the Measurement Scale was set to Custom. The cross-sectional area was determined in mm^2 as per an existing methodology.[7]

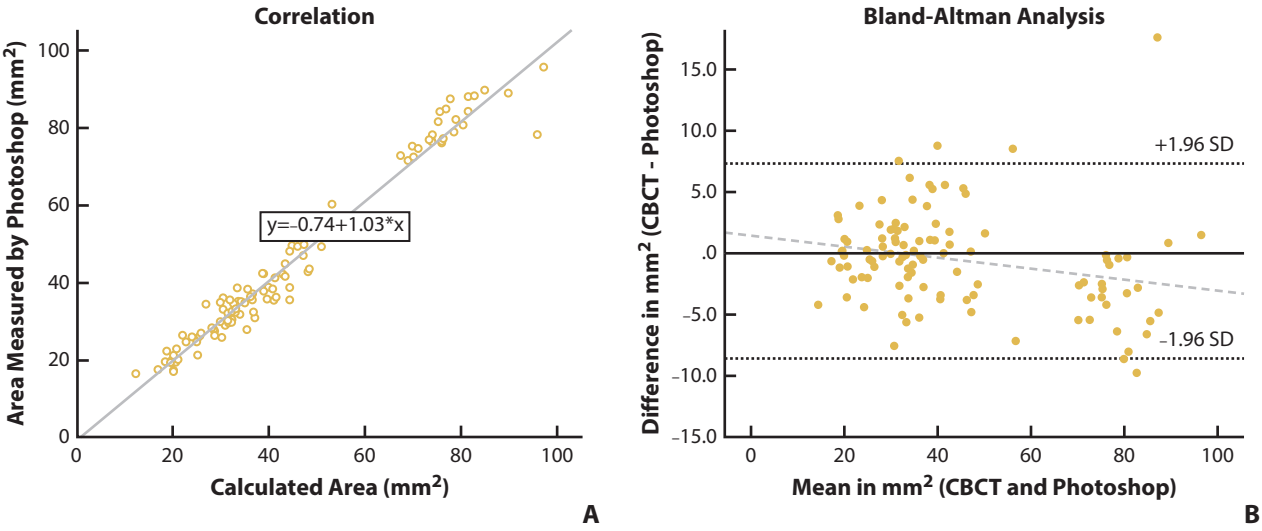

Figure 2. A, Regression line indicating strong correlation (r=0.9) and small bias between simplified formula calculated area (x-axis) and area measured directly in photo-editing software program. B, Agreement between 2 methods demonstrated by Bland-Altman analysis. Mean bias (-0.61 mm^2) indicated by solid line. Dotted lines indicate 2 Limit of Agreements (-8.57 mm^2 to 7.36 mm^2). Positive trend of regression line (dashed line) indicates proportional bias (r=-0.24, *P*<.012). At higher area, direct method gave slightly higher readings than algorithm. CBCT, cone beam computed tomography.

The cross-sectional area was defined with the Lasso Tool. The Record Measurements function of the software was then used to calculate the area of the cross section.

The data in the text and tables are given by mean, standard error, and 95% confidence intervals. The strength in the relationship between the area measured by the photo-editing software program and the area calculated by the simplified formula was estimated by the Pearson correlation coefficient (R) and determined by the linear mixed model.[28,29] The agreement between the 2 methods was evaluated based on Bland-Altman analysis, calculating the limits of agreement.[30]

The mean estimates of the parameters and the difference between them were calculated by the linear mixed model with restricted maximum likelihood estimation. The 3 parameters (a, b, c) were analyzed in separate mixed models for anterior and premolar teeth. For molars, 4 models were run (a, b, h1, h2). The fixed factor was the tooth type with 10 levels for anterior and premolar teeth (5 maxillary and 5 mandibular tooth types), and 4 levels (2 maxillary and 5 mandibular tooth types) for molars. In a preliminary analysis, no differences were found between the left and right teeth. Therefore, the "side" was considered as a random factor. The random intercept accounts for the participant ID ("subject"). Pairwise comparisons were made separately for each molar parameter and separately for each anterior and premolar parameter by the least significant difference post hoc test. The *P* values were adjusted by the Bonferroni method. Two teeth were put into the same parameter cluster if no significant differences were found between them for a specific parameter. If neither parameter (4 for molars and 3 for the other teeth) were different for 2 teeth, they were put into the same abutment cluster. The abutment clusters determined the type of anatomic healing abutment. All statistical analyses were performed with a statistical software program (IBM SPSS Statistics, v25; IBM Corp).

RESULTS

The mean area of the cervical cross sections measured by the photo-editing software program (45.6 ±4.4 mm^2) was not significantly different from the mean area calculated by the simplified formula from the parameters measured on CBCT images (45.0 ±4.1 mm^2, *P*=.224), indicating low bias (-0.61 ±0.49 mm^2) between methods. A strong significant correlation was found between the 2 measurements (r=0.90, *P*<.001) (Fig. 2A). The upper and lower limits of agreement were -8.57 mm^2 and 7.36 mm^2, respectively. The significant proportional bias (r=-0.24, *P*<.012) indicated that, at the higher area, the direct method resulted in slightly higher readings than the calculation formula (Fig. 2B).

The means of the 3 parameters (a, b, c) for anterior, canine, and premolar teeth are shown in Table 1. The table also indicates the parameter cluster based on the statistical differences (*P*<.001) among the teeth within a parameter. For the common clusters, grouped means were calculated (7 for the a, 3 for the b, 4 for the c). After clustering the teeth in all the 3 parameters, 9 possible healing abutment anatomies were determined for the 10 tooth types (Table 2).

Table 1. Parameters for the anterior, canine, and premolars teeth (in mm)

Parameter	Arch	Tooth	Mean	SE	95% CI		Parameter Cluster		Grouped Mean
					Lower	Upper	A	B	
"a"	Mandibular	Central incisor	3.5	0.069	3.3	3.6	1	–	3.5
		Lateral incisor	3.9	0.068	3.8	4.0	2	–	3.9
		Canine	5.2	0.068	5.0	5.3	3	–	5.2
		First premolar	5.2	0.070	5.1	5.4	3	–	–
		Second premolar	5.4	0.075	5.3	5.6	4	1	5.4
	Maxillary	Central incisor	6.2	0.076	6.0	6.3	5	–	6.2
		Lateral incisor	4.8	0.073	4.7	5.0	6	–	4.8
		Canine	5.8	0.071	5.6	5.9	7	–	5.8
		First premolar	5.2	0.074	5.0	5.3	3	–	–
		Second premolar	5.3	0.080	5.1	5.4	3	1	–
"b"	Mandibular	Central incisor	3.9	0.088	3.7	4.1	1	–	3.9
		Lateral incisor	4.0	0.087	3.8	4.2	1	–	–
		Canine	5.1	0.086	5.0	5.3	2	–	5.2
		First premolar	4.6	0.090	4.4	4.8	3	–	4.7
		Second premolar	4.5	0.101	4.3	4.7	3	–	–
	Maxillary	Central incisor	4.5	0.103	4.3	4.7	3	–	–
		Lateral incisor	3.9	0.098	3.7	4.1	1	–	–
		Canine	5.2	0.094	5.0	5.3	2	–	–
		First premolar	5.4	0.099	5.2	5.6	2	–	–
		Second premolar	5.1	0.113	4.9	5.3	2	–	–
"c"	Mandibular	Central incisor	1.9	0.091	1.7	2.1	1	–	2.1
		Lateral incisor	2.3	0.090	2.1	2.4	2	–	2.4
		Canine	2.6	0.088	2.5	2.8	3	2	2.6
		First premolar	2.9	0.093	2.7	3.1	3	–	–
		Second premolar	3.4	0.103	3.2	3.6	4	–	3.0
	Maxillary	Central incisor	2.2	0.105	2.0	2.4	1	2	–
		Lateral incisor	2.5	0.100	2.3	2.7	2	3.1	–
		Canine	3.0	0.096	2.8	3.2	3	–	–
		First premolar	3.5	0.101	3.3	3.7	4	–	–
		Second premolar	3.9	0.114	3.6	4.1	4	–	–

The means of the 4 parameters (a, b, h_1, and h_2) for molar teeth are shown in Table 3. The table also indicates the parameter cluster based on the statistical differences ($P<.001$) among teeth within a parameter. For the common cluster, grouped means were calculated (2 for the a, 2 for the b, 1 for the h_1, 2 for the h_2). After clustering the teeth in all 4 parameters, 3 possible healing abutment anatomies were determined for the 4 tooth types (Table 4).

The comparison cross-sectional diameters with the results of other studies are shown in Table 5. The buccolingual diameters of the anterior, canine, and premolar teeth (parameter h) were calculated by adding c to b, while the mesiodistal diameters coincided with parameter a. The buccolingual diameters of the molars were calculated from the mean of the larger (parameter a) and the smaller diameter (parameter b). The mesiodistal diameter h was the sum of parameters h_1 and h_2.

Table 2. The clusters of the healing abutment for the anterior teeth and premolars

Arch	Tooth	Mean of the Parameters			Healing Abutment Cluster
		a	b	c	
Mandibular	Central incisor	3.5	3.9	2.1	1
	Lateral incisor	3.9		2.4	2
	Canine	5.2	5.2	2.6	3
	First premolar				4
	Second premolar	5.4	4.7	3.0	5
Maxillary	Central incisor	6.2		2.1	6
	Lateral incisor	4.8	3.9	2.4	7
	Canine	5.8		2.6	8
	First premolar	5.2	5.2	3.0	9
	Second premolar				9

DISCUSSION

This study introduces a novel method of defining the geometry of the cross-sectional area of human teeth at the level of the CEJ by using a simplified mathematical formula. The cross-sectional areas calculated with the formula correlated highly to the actual cross-sectional areas that were measured directly. This correlation suggests that the novel mathematical formula can be

Table 3. Parameters for the molars (in mm)

Parameter	Arch	Tooth	Mean	SE	95% CI		Parameter-Cluster	Grouped Mean
					Mandibular	Maxillary		
"a"	Mandibular	First molar	9.4	0.151	9.1	9.7	1	9.4
	–	Second molar	9.3	0.139	9.0	9.6	1	–
	Maxillary	First molar	10.8	0.139	10.6	11.1	2	10.8
	–	Second molar	10.7	0.134	10.5	11.0	2	–
"b"	Mandibular	First molar	8.9	0.163	8.6	9.3	1	8.8
	–	Second molar	8.6	0.150	8.3	8.9	1	–
	Maxillary	First molar	9.9	0.150	9.6	10.2	2	9.8
	–	Second molar	9.7	0.145	9.4	10.0	2	–
"h_1"	Mandibular	First molar	2.4	0.105	2.2	2.6	1	2.4
	–	Second molar	2.5	0.095	2.3	2.6	1	–
	Maxillary	First molar	2.5	0.095	2.3	2.6	1	–
	–	Second molar	2.4	0.091	2.3	2.6	1	–
"h_2"	Mandibular	First molar	6.6	0.145	6.3	6.9	1	6.7
	–	Second molar	6.9	0.131	6.6	7.1	1	–
	Maxillary	First molar	6.5	0.132	6.2	6.7	1	–
	–	Second molar	6.1	0.126	5.8	6.3	2	6.1

confidently used to predict the cervical tooth cross-sectional geometry.

The parameters required to define the cross-sectional area can be readily measured on a CBCT scan, which facilitates a rapid and highly precise calculation. Anteriors, canines, and premolars require only 3 parameters, while molars need 4 parameters. This simplified approach may also facilitate the design of prefabricated, tooth-specific healing abutments and/or their custom manufacture by computerized numerical control or 3-dimensional printing. Based on the measurements, prototypes of a series of anatomic healing abutment were designed and presented in Figure 3. The vertical transition from the cylindrical narrower implant platform to the wider coronal area with anatomically shaped horizontal cross section was designed to be smooth and gently S-shaped.[31] However, analyzing the significance of vertical dimension, gingival biotypes, and bone thickness was beyond the scope of this study.

Significant differences between parameters defined clusters. However, statistical significance is determined by the effect size, which depends on the differences between 2 means and the standard deviation. Therefore, both measurement precision and biologic variation may affect results. In the present study, the minimum difference to define separate clusters in at least one parameter was 0.38 mm (between mandibular canines and maxillary first premolars and between mandibular first and second premolars). Further clinical tests may help optimize the process by reducing the number of custom abutments required to cover the variability in shapes and sizes observed in the natural dentition.

Previous data regarding the cross-sectional size and geometry of teeth for a white population are sparse. To compare with earlier studies, mesiodistal and buccolingual diameters were calculated from the measured parameters (an oversimplification of the geometry). Sun et al[7] measured the diameters of 28 teeth in 30 healthy Chinese volunteers aged 18 to 25 years with a complete dentition from CBCT scans. These measurements were made 1.5-mm apical to the alveolar ridge crest, possibly explaining the generally lower values of the cross-sectional area. The large difference (>1 mm) observed in the buccolingual diameters of maxillary and mandibular second premolars and mandibular molars and in the mesiodistal diameter of maxillary molars may be from population or ethnical differences. Nose et al[25] measured 106 skulls in India, measuring diameters at the CEJ. These results are closer to those of the present study, except the mesiodistal diameters of the maxillary molars, which were higher by 1.6 to 1.7 mm. A study of 71 Japanese skulls[8] measured at the CEJ reported good consistency with the present study, except for the higher maxillary first molar mesiodistal diameter. Other explanations for the differences may include measurement techniques (calipers on cadavers versus from CBCT scans, CEJ versus root cross section) and ethnic variability. The molar deviation was the most significant and

Table 4. The clusters of the healing abutment for molars

Arch	Tooth	Mean of the Parameters				Healing Abutment Cluster
		a	b	h_1	h_2	
Mandibular	First molar	9.4	8.8	2.4	6.7	1
–	Second molar					1
Maxillary	First molar	10.8	9.8			2
–	Second molar				6.1	3

Table 5. Comparison of the present study's diameters to other studies

			Present Study	[7]		[25]		[8]	
Aspect	**Tooth**	**Arch**	**Caucasian**	**Chinese**	**Difference**	**South Asian**	**Difference**	**Japanese**	**Difference**
Mesiodistal	Central incisor	Mandibular	3.5	3.3	0.2	3.42	0.0	3.6	-0.2
		Maxillary	6.2	5.0	1.1	6.11	0.0	6.4	-0.2
	Lateral incisor	Mandibular	3.9	3.6	0.3	3.73	0.2	4.0	-0.1
		Maxillary	4.8	4.3	0.5	4.82	0.0	5.1	-0.3
	Canine	Mandibular	5.2	5.1	0.0	5.26	-0.1	5.4	-0.2
		Maxillary	5.8	5.4	0.4	5.62	0.1	5.9	-0.1
	First premolar	Mandibular	5.2	4.6	0.7	4.89	0.3	5.1	0.1
		Maxillary	5.2	4.4	0.8	4.81	0.3	5.1	0.0
	Second premolar	Mandibular	5.4	4.7	0.8	5.03	0.4	5.3	0.2
		Maxillary	5.2	4.4	0.9	4.74	0.5	5.1	0.2
	First molar	Mandibular	9.0	8.9	0.1	8.84	0.2	9.2	-0.2
		Maxillary	9.4	7.0	2.4	7.67	1.7	8.1	1.3
	Second molar	Mandibular	9.0	9.1	-0.1	8.89	0.1	9.6	-0.7
		Maxillary	9.1	7.3	1.8	7.49	1.6	8.2	0.9
Buccolingual	Central incisor	Mandibular	5.8	6.0	-0.2	5.55	0.3	5.6	0.2
		Maxillary	6.7	6.7	0.0	6.59	0.1	6.6	0.1
	Lateral incisor	Mandibular	6.2	6.6	-0.3	6.09	0.1	6.2	0.1
		Maxillary	6.4	6.1	0.3	6.22	0.1	6.2	0.1
	Canine	Mandibular	7.8	8.0	-0.3	7.54	0.2	7.6	0.2
		Maxillary	8.1	7.9	0.3	7.94	0.2	8.0	0.1
	First premolar	Mandibular	7.5	6.7	0.7	7.1	0.4	7.1	0.4
		Maxillary	8.8	8.5	0.4	8.54	0.3	8.7	0.2
	Second premolar	Mandibular	7.9	6.9	1.0	7.28	0.6	7.3	0.6
		Maxillary	9.0	8.0	1.0	8.48	0.5	8.6	0.3
	First molar	Mandibular	9.4	7.6	1.7	9.41	-0.1	9.4	0.0
		Maxillary	10.8	10.5	0.3	10.71	0.1	10.8	0.0
	Second molar	Mandibular	9.3	7.7	1.6	9.53	-0.3	9.7	-0.4
		Maxillary	10.7	10.6	0.1	10.84	-0.1	11.1	-0.3

may suggest that white people may have a larger cervical cross-sectional area than Asian individuals.

Limitation of the present study included that only the teeth of white people were measured; thus, future research should aim to expand the measurement for other populations. The present study was limited to defining horizontal cervical geometry at the buccal CEJ level to simplify the horizontal cross-section calculations, although the CEJ is not 2 dimensional but 3 dimensional. This study could be a good basis for understanding cervical teeth anatomy. Nevertheless, further investigation would be necessary to define the differences in facial and proximal CEJ positions, which are essential to developing an appropriate emergence profile, especially for anterior maxillary teeth and immediate implant placement. An anatomic prefabricated abutment system could be more suitable for partially or fully edentulous arches when a schematic but anatomic-like abutment facilitates the workflow. In the replacement of a single anterior tooth, further individualization might be necessary to incorporate the variation in interdental, vertical, and surface dimensions.

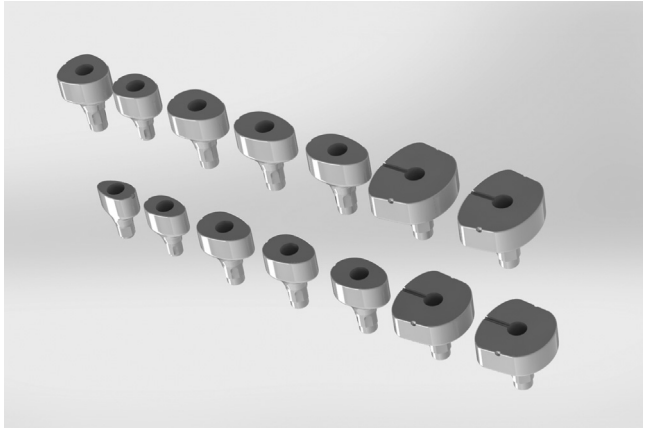

Figure 3. Schematic drawing of prototypes of anatomic healing abutment designed for various tooth types.

CONCLUSIONS

Based on the findings of this in vitro study, the following conclusions were drawn:

1. The developed mathematical algorithm represents the cross-sectional geometry of the tooth type at the CEJ with high accuracy.
2. The parameters used for this formula can be readily applied and can precisely measure cervical geometry for comparison studies.
3. The most important clinical application of this novel mathematical algorithm is its ability to shape, size, and design the horizontal dimension of accurate anatomic healing abutments.
4. A set of 12 healing abutments could cover all the possible dimensions of the horizontal cross sections in the dentition of white individuals.

REFERENCES

1. TheInsightPartners. Dental implants market to 2027 - global analysis and forecasts by product; material; end user and geography. Dublin 2019. Available at: https://www.businesswire.com/news/home/20190411005716/en/Dental-Implants-Market-to-2027—Global-Analysis-Forecasts-by-Product-Material-End-User-and-Geography—ResearchAndMarkets.com. Accessed April 11, 2019.
2. Hermann JS, Buser D, Schenk RK, Higginbottom FL, Cochran DL. Biologic width around titanium implants. A physiologically formed and stable dimension over time. Clin Oral Implants Res 2000;11:1-11.
3. Berglundh T, Lindhe J. Dimension of the periimplant mucosa. Biological width revisited. J Clin Periodontol 1996;23:971-3.
4. Smukler H, Castellucci F, Capri D. The role of the implant housing in obtaining aesthetics: generation of peri-implant gingivae and papillae–part 1. Pract Proced Aesthet Dent 2003;15:141-9; quiz 50.
5. Buser D, Martin W, Belser UC. Optimizing esthetics for implant restorations in the anterior maxilla: anatomic and surgical considerations. Int J Oral Maxillofac Implants 2004;19 Suppl:43-61.
6. Su H, Gonzalez-Martin O, Weisgold A, Lee E. Considerations of implant abutment and crown contour: critical contour and subcritical contour. Int J Periodontics Restorative Dent 2010;30:335-43.
7. Sun M, Gu F, Wang J, Zhou C, Xia J, Qin H, et al. Measurement for natural dental neck data of normal adults and its clinical significance on guiding implant restoration. Int J Clin Exp Med 2015;8:14732-40.
8. Tomuro M, Watanabe F, Takase I, Hata Y. Measurements of cervical dimensions of Japanese teeth for selecting implant diameter. J Jpn Soc Oral Implantol 2010;23:12-7.
9. Bichacho N, Landsberg CJ. Single implant restorations: prosthetically induced soft tissue topography. Pract Periodontics Aesthet Dent 1997;9:745-52; quiz 54.
10. Lee EA. Transitional custom abutments: optimizing aesthetic treatment in implant-supported restorations. Pract Periodontics Aesthet Dent 1999;11:1027-34; quiz 36.
11. Steigmann M, Monje A, Chan HL, Wang HL. Emergence profile design based on implant position in the esthetic zone. Int J Periodontics Restorative Dent 2014;34:559-63.
12. Chee WW, Donovan TE. Treatment planning and soft tissue management for optimal implant aesthetics. Ann Acad Med Singap 1995;24:113-7.
13. Bishti S, Strub JR, Att W. Effect of the implant-abutment interface on peri-implant tissues: a systematic review. Acta Odontol Scand 2014;72:13-25.
14. Fazekas R, Molnar E, Nagy P, Mikecs B, Windisch P, Vag J. A proposed method for assessing the appropriate timing of early implant placements: a case report. J Oral Implantol 2018;44:378-83.
15. Hammerle CH, Chen ST, Wilson TG Jr. Consensus statements and recommended clinical procedures regarding the placement of implants in extraction sockets. Int J Oral Maxillofac Implants 2004;19 Suppl:26-8.
16. Cooper LF. Objective criteria: guiding and evaluating dental implant esthetics. J Esthet Restor Dent 2008;20:195-205.
17. Wittneben JG, Buser D, Belser UC, Bragger U. Peri-implant soft tissue conditioning with provisional restorations in the esthetic zone: the dynamic compression technique. Int J Periodontics Restorative Dent 2013;33:447-55.
18. Parpaiola A, Sbricoli L, Guazzo R, Bressan E, Lops D. Managing the peri-implant mucosa: a clinically reliable method for optimizing soft tissue contours and emergence profile. J Esthet Restor Dent 2013;25:317-23.
19. Monaco C, Evangelisti E, Scotti R, Mignani G, Zucchelli G. A fully digital approach to replicate peri-implant soft tissue contours and emergence profile in the esthetic zone. Clin Oral Implants Res 2016;27:1511-4.
20. Alani A, Corson M. Soft tissue manipulation for single implant restorations. Br Dent J 2011;211:411-6.
21. Munksgaard EC, Peutzfeldt A, Asmussen E. Elution of TEGDMA and BisGMA from a resin and a resin composite cured with halogen or plasma light. Eur J Oral Sci 2000;108:341-5.
22. Hensten-Pettersen A. Skin and mucosal reactions associated with dental materials. Eur J Oral Sci 1998;106:707-12.
23. Daftary F. The bio-esthetic abutment system: an evolution in implant prosthetics. Int J Dent Symp 1995;3:10-5.
24. Daftary F. Dentoalveolar morphology: evaluation of natural root form versus cylindrical implant fixtures. Pract Periodontics Aesthet Dent 1997;9:469-77; quiz 78.
25. Nose H, Tawada Y, Watanabe F, Kageyama I. Comparison of diameters at the cementoenamel junction between South Asians and Japanese. Odontology 2011;99:22-7.
26. Nelson SJ. Wheeler"s dental anatomy, physiology, and occlusion. 11th ed. St. Louis: Elsevier Health Sciences; 2019. p. 90-189.
27. Suresh K. An overview of randomization techniques: an unbiased assessment of outcome in clinical research. J Hum Reprod Sci 2011;4:8-11.
28. Hamlett A, Ryan L, Serrano-Trespalacios P, Wolfinger R. Mixed models for assessing correlation in the presence of replication. J Air Waste Manag Assoc 2003;53:442-50.
29. Gánti B, Bednarz W, Kőműves K, Vág J. Reproducibility of the PIROP ultrasonic biometer for gingival thickness measurements. J Esthet Restor Dent 2019;31:263-7.
30. Bland JM, Altman DG. Measuring agreement in method comparison studies. Stat Methods Med Res 1999;8:135-60.
31. Schoenbaum TR, Chang YY, Klokkevold PR, Snowden JS. Abutment emergence modification for immediate implant provisional restorations. J Esthet Restor Dent 2013;25:103-7.

Corresponding author:
Dr János Vág
Department of Conservative Dentistry
Semmelweis University
Szentkirályi utca 47, Budapest H-1088
HUNGARY
Email: drvagjanos@gmail.com

Acknowledgments
The authors thank dental students Fanni Andrea Puskás and Máté Zámodics for their assistance in collecting data. Thanks for the engineer, Zoltán Nagy for designing and technical drawing of the anatomical healing abutment prototype. The "Design Of Prefabricated Anatomical Healing Abutments Based On Physiological Measurements" patent application is filed into Hungarian Intellectual Property Office in 03/Oct/2019.

CRediT authorship contribution statement
János Vág: Formal analysis, Validation, Project administration, Funding acquisition, Writing - original draft. **George Freedman:** Writing - review & editing. **Enikő Szabó:** Visualization, Writing - review & editing. **László Románszky:** Conceptualization, Methodology. **Gábor Berkei:** Conceptualization, Methodology, Investigation.

https://doi.org/10.1016/j.prosdent.2020.11.023